Available online at www.sciencedirect.com
ScienceDirect
Journal of Catalysis 245 (2007) 381–391
JOURNAL OF CATALYSIS
www.elsevier.com/locate/jcat

Transesterification of triacetin with methanol on Nafion® acid resins

Dora E. López, James G. Goodwin Jr. *, David A. Bruce

Department of Chemical and Biomolecular Engineering, Clemson University, Clemson, SC 29634, USA

Received 12 June 2006; revised 24 October 2006; accepted 30 October 2006

Available online 29 November 2006

Abstract

Although homogeneous alkali catalysts (e.g., NaOH) are commonly used to produce biodiesel by transesterification of triglycerides (vegetable oils and animal fats) and methanol, solid acid catalysts, such as acidic resins, are attractive alternatives because they are easy to separate and recover from the product mixture and also show significant activity in the presence of fatty acid impurities, which are common in low-cost feedstocks. To better understand solid acid catalyst performance, a fundamental transesterification kinetic study was carried out using triacetin and methanol on Nafion® (perfluorinated-based ion-exchange resin) catalysts. In particular, Nafion® SAC-13 (silica-supported Nafion) and Nafion® NR50 (unsupported Nafion) were investigated, because both show great promise for biodiesel-forming reactions. The reaction kinetics for a common homogeneous acid catalyst (H_2SO_4) were also determined for comparison. Liquid-phase reaction was performed at 60 °C using a stirred batch reactor. The swelling properties of the resin in solvents of diverse polarity that reflect solutions typically present in a biodiesel synthesis mixture were examined. The initial reaction rate was greatly affected by the extent of swelling of the resin, where, as expected, a greater effect was observed for Nafion® NR50 than for the highly dispersed Nafion® SAC-13. The reaction orders for triacetin and methanol on Nafion® SAC-13 were 0.90 and 0.88, respectively, similar to the reaction orders determined for H_2SO_4 (1.02 and 1.00, respectively). The apparent activation energy for the conversion of triacetin to diacetin was 48.5 kJ/mol for Nafion® SAC-13, comparable to that for H_2SO_4 (46.1 kJ/mol). Selective poisoning of the Brønsted acid sites on Nafion® SAC-13 using pyridine before transesterification revealed that only one site was involved in the rate-limiting step. These results suggest that reaction catalyzed by the ion-exchange resin can be considered to follow a mechanism similar to that of the homogeneous catalyzed one, where protonated triglyceride (on the catalyst surface) reaction with methanol is the rate-limiting step.

Keywords: Biodiesel; Triacetin; Methanol; Transesterification; Sulfonic acid resins; Nafion® SAC-13; Nafion® NR50; Polymer swelling; H_2SO_4

1. Introduction

Recent concerns about the increasing cost of petroleum-derived fuels have excited interest in the production of renewable fuels, especially biodiesel. Biodiesel consists of fatty acid alkyl esters that are commonly derived from vegetable oils. Conversion of these oils, consisting primarily of triglycerides, to biodiesel fuel is commonly achieved through a series of transesterification reactions involving the reaction of an alkoxy group of an ester (i.e., mono-, di-, or triglyceride) with that of a small alcohol (e.g., methanol or ethanol). This reaction has traditionally been catalyzed by homogeneous catalysts, such as alkaline bases or mineral acids [1–6]. However, environmental and economic concerns are such that a continuous process that uses a heterogeneous catalyst is much more desirable. In particular, solid acid catalysts are ideal because they are able to catalyze both transesterification and esterification reactions simultaneously, which becomes important when using lower-quality feedstocks (e.g., used deep-frying oils) [7–9].

Sulfonic resins compose a group of acid catalysts that can be classified according to the polymer backbone, namely polystyrene (e.g., Amberlyst® resins) or perfluorinated alkanes (e.g., Nafion® resins) [10]. These acid resins have inherently low surface areas unless a solvent is used to swell the polymer, thereby exposing additional internal acid sites for reaction. Because high surface areas are more desirable for heterogeneous catalysis, increased polymer surface area (without relying on solvent swelling) can be achieved by supporting these polymers on inert high-surface area oxide materials. For example, Nafion® SAC-13 is a highly acidic Nafion®–

* Corresponding author. Fax: +1 864 656 0784.
E-mail address: james.goodwin@ces.clemson.edu (J.G. Goodwin Jr.).

0021-9517/$ – see front matter
doi:10.1016/j.jcat.2006.10.027

Table 1
Physicochemical characteristics of Nafion® SAC-13 and Nafion® NR50

Parameter	Nafion® SAC-13	Nafion® NR50
Support	SiO_2	None
Composition	Fluorosulfonic acid Nafion® polymer (10–20 wt%) on amorphous silica (porous nanocomposite)[a]	Fluorosulfonic acid Nafion® polymer
Acidic group	$–CF_2CF_2SO_3H$	$–CF_2CF_2SO_3H$
Ionic form	H^+	H^+
Exchange capacity	150 μeq/g[b] (120–1000 μeq/g)[a]	⩾800 μeq/g[a] (>90%)[b]
Pellet shape	Lobular, lengthwise striations	Cylindrical and spherical
Pellet size	+20 mesh (diameter ∼1 mm, length/diameter = 9.4)[c]	7–9 mesh (1.6–2.8 mm)[d]
Pore volume	>0.6 mL/g[a]	N/A
Pore diameter	>10 nm[a]	N/A
Bulk density	0.4–0.5 g/mL[a]	N/A
Polymer density	2.1 g/mL[a]	2.1 g/mL[a]
Surface area	>200 m^2/g[a]	–

[a] General information provided by the manufacturer.
[b] Specific information provided by the manufacturer for the Nafion® NR50 utilized (batch # 04601MB).
[c] Specific information provided by the manufacturer for the Nafion® SAC-13 utilized (batch # 05729PC).
[d] Catalyst not swelled.

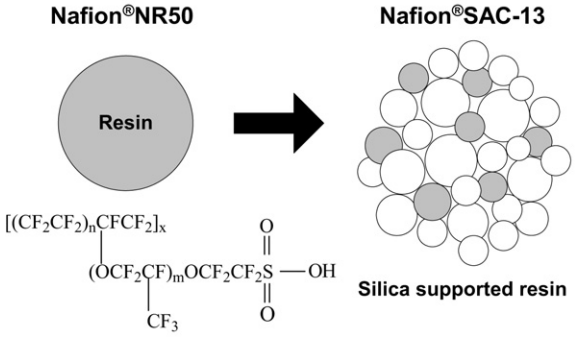

Fig. 1. Schematic of the Nafion® catalysts: $m = 1$, 2 or 3, $n = 6$–7, and $x \sim 1000$. Redrawn from Ref. [11].

silica nanocomposite (Fig. 1) that contains 13 wt% Nafion, which is a copolymer of tetrafluoroethylene and perfluoro-2-(fluorosulfonylethoxy)propyl vinyl ether. The small (5–30 nm) Nafion® resin particles [11] are entrapped within the porous silica matrix. This acid catalyst has been shown to effectively catalyze numerous industrial reactions, including olefin isomerizations, alkylations, acylations, oligomerizations, esterifications, and others [11–13]. A more detailed list of the physicochemical properties of this type of catalyst is provided in Table 1.

Although the use of solid acid catalysts for the continuous production of biodiesel is promising, only limited information exists about triglyceride transesterification rates or the extent of catalyst deactivation [7,14–18]. We previously reported, based on turnover frequency (TOF) results, that solid acid catalysts, such as Nafion® NR50, sulphated zirconia (SZ), and tungstated zirconia (WZ), have sufficient acid site strength to catalyze biodiesel-forming transesterification reactions as efficiently as sulfuric acid [15]. In the same study, Nafion® NR50 was found to give higher selectivity to final products (methyl ester and glycerol) compared with other solid acid catalysts. Because of the significant acid strength and selectivity of Nafion® NR50 and improved surface area of Nafion® SAC-13 (without relying on solvent swelling), these catalysts were chosen for more detailed kinetic and mechanistic studies of the liquid-phase transesterification of triacetin ($C_9H_{14}O_6$) and methanol. Reaction catalyzed by sulfuric acid was also studied for comparison. All three catalysts have only Brønsted acid sites. The consecutive transesterification reactions occurring in the conversion of triacetin to diglycerides, monoglycerides, glycerol, and esters have been illustrated elsewhere [15]. Triacetin was used as a model triglyceride for the detailed kinetic study because it can be obtained in a pure form and has all carboxylic side groups identical (acetic acid), thereby facilitating the kinetic analysis of reaction. Although there is a decrease in reaction rate as the carboxylic acid side groups grow larger, preliminary results have shown that the reaction rates of small triglycerides are directly related to those of much larger triglycerides.

2. Experimental

2.1. Materials

Nafion® SAC-13, Nafion® NR50, triacetin (99.5 wt%), methanol (99.9 wt%), acetic acid (99.7 wt%), tetrahydrofuran (99.9 wt%), pyridine (99+ wt%), methyl acetate (99 wt%), acetins mixture (45 wt% diacetin, 26 wt% monoacetin, 25 wt% triacetin, and 4 wt% glycerol), and refined olive oil (low acidity) were purchased from Sigma-Aldrich and used as received. Ethanol solvent (99.5 wt%), toluene (99.8 wt%) internal standard, and H_2SO_4 (95–98 wt%) were obtained from Acros Organics, Fisher Scientific, and EMD, respectively.

2.2. Catalyst characterization

So as to be able to relate the observed kinetic behavior with catalyst properties, several analytical techniques were used to probe relevant physicochemical properties of the Nafion® SAC-13 and Nafion® NR50 catalysts studied. Catalyst total surface area (S_{BET}) was determined by BET analysis as described previously [15]. Analogous conditions were used here to determine pore volume and average pore size in a Micromeritics ASAP 2020 instrument.

The number of catalytically available acid sites was determined by titration, chemisorption, and elemental analysis methods. The titration technique involved an ion-exchange step, in which 0.2 g of catalyst was added to 10 mL of a 3.42 M aqueous solution of NaCl under stirring. After 30 h of ion exchange at 28 °C between the catalyst H^+ ions and the Na^+ ions in solution, the liquid was filtered off and titrated with a 0.05 N aqueous NaOH solution. The endpoint for titration was determined using a pH meter (pH ∼ 7) and corroborated using pH paper. Pulse NH_3 chemisorption using an Altamira AMI-1 was also used to quantify the number of surface-exposed acid sites present in Nafion® SAC-13 and in Nafion® NR50 [15]. Finally, the total number of acid sites (available and inaccessible) was determined by elemental sulfur analysis using a combustion technique in which the sample was heated to ∼1000 °C and IR was used to quantify the resulting SO_3 (Galbraith Laboratory, Knoxville, TN).

Catalyst resin load, thermal stability, and degradation behavior were determined by thermogravimetric analysis using a Pyris 1 TGA (Perkin–Elmer). Sample weight changes were recorded as the Nafion® SAC-13 (∼8 mg) or the Nafion® NR50 (∼20 mg) catalyst was heated at a rate of 15 °C/min from room temperature to 700 °C under both nitrogen and air atmospheres.

The resin–silica nanocomposite morphology of Nafion® SAC-13 was studied using a Hitachi S-4700 scanning electron microscope. Before analysis, the samples were mounted on carbon stubs using double-stick adhesive tape. The samples were then coated with a thin layer of platinum in a Hummer 6.2 sputtering unit to prevent sample charging during SEM analysis. Finally, SEM digital images were collected with the electron beam kept at 5 kV.

2.3. Reaction studies

Before reaction, Nafion® SAC-13 pellets were ground and sieved to get the desired particle size, and then dried at 90 °C overnight under a partial vacuum of 280 Torr. Nafion® NR50 and H_2SO_4 were used as received. Unless otherwise specified, the catalyst was added dry to the reaction mixture to start the reaction. The transesterification reaction rates were investigated using an isothermal, well-mixed batch reactor (Parr model 4590). Typically, the 100 mL stainless steel (316 SS) reactor was filled with approximately 49 g of the reagent solution, which contained methanol and triacetin in a 6:1 molar ratio (13.8 M methanol and 2.3 M triacetin, respectively). The reactants were then heated to the desired temperature, and the solid catalyst (1 g) or H_2SO_4 (0.022 g) was added shortly after the reactor temperature reached steady state, so as to initiate the reaction. Initial reaction rate kinetics were measured for triacetin conversion <5%. Sample aliquots (0.1 mL) were withdrawn periodically from the reactor, quenched to room temperature, and centrifuged to separate out the solid catalyst to prevent further reaction. For the reference experiments using H_2SO_4 as the catalyst, the samples were placed in an ice bath before GC analysis. To evaluate catalyst deactivation, the same batch of solid catalyst (Nafion® SAC-13) was reused several times. In experiments where the initial concentrations of reactants were varied to determine the power rate law, tetrahydrofuran (THF) was used as an inert diluent [19]. Reaction sample concentrations were determined using an HP 6890 gas chromatograph equipped with flame ionization detector and splitless mode injector as previously reported [15]. Solutions of known concentration of reactants and products were used for determination of multipoint GC calibration curves. The effect of stirrer speed and the presence/absence of diffusion effects on the reaction kinetics were investigated and are described below.

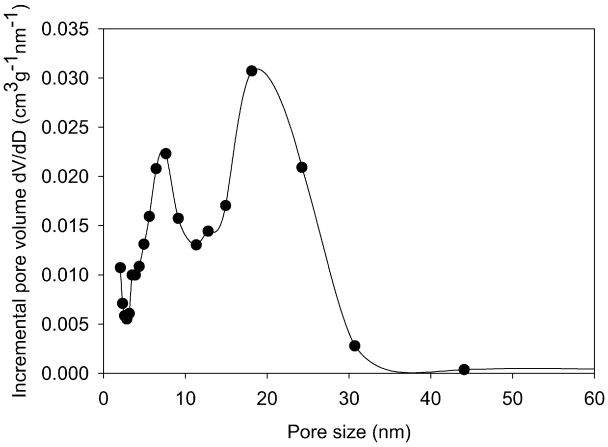

Fig. 2. Pore size distribution of Nafion® SAC-13 (vacuum dried at 90 °C).

3. Results and discussion

3.1. Solid catalyst characterization

3.1.1. Catalyst surface area and pore size distribution

For Nafion® SAC-13, the measured BET surface area and pore volume were 221 ± 20 m^2/g and 0.56 ± 0.01 mL/g, respectively (identical within experimental error for ground and pellet forms of the catalyst). These results are in the range of previously reported BET surface areas of 150–500 m^2/g [13,20]. In addition, these results compare well with the data provided by the manufacturer (200 m^2/g and 0.60 mL/g). As shown in Fig. 2, Nafion® SAC-13 exhibited a bimodal distribution of the pores with average pore diameters of 8 and 19 nm. Nafion® NR50, on the other hand, is known to have a nonporous structure when dry [10,21]; thus, it exhibited an extremely low surface area (<1 m^2/g) in the unswelled state [13].

3.1.2. Nafion® swelling properties

Here, only Nafion® NR50 was studied, because it is difficult to distinguish between any slight pore volume changes in the supported resin and the permanent pore volume of the matrix in Nafion® SAC-13. The swelling properties of the dried Nafion® resin in different solvents (i.e., methanol, water, and triglyceride) were examined. Swelling in water was investigated, because it may be present in lower-quality biodiesel feedstocks (before or during biodiesel synthesis). Because our final goal is to understand the kinetics of transesterification of vegetable oils, a highly refined olive oil (acid value = 0.04) also was used here as a solvent for comparison. The catalyst particle dimensions (obtained with a vernier caliper) and weights were

Table 2
Results and calculated values for Nafion® NR50 volume increase in different solvents

Solvent	$\Delta l/l$[a]	$\Delta d/d$[b]	$\Delta V/V$ (%)		
			Based on pellet dimensions	Based on Eq. (1)	From the literature [22]
Methanol	46 ± 7	47 ± 4	436 ± 108	429 ± 37	209
Water	14 ± 0	16 ± 3	60 ± 10	68 ± 1	43
Triacetin	1 ± 7	5 ± 9	15 ± 29	20 ± 6	–
Olive oil	5 ± 5	2 ± 5	9 ± 12	12 ± 8	–

[a] l = pellet length.
[b] d = pellet diameter.

measured for several Nafion® NR50 cylindrical-shaped pellets before and after soaking in the pure solvent at 60 °C (typical transesterification reaction temperature) until equilibrium was reached. Irreversible swelling after cooling has been proved to be a good assumption for this type of system [22]. The volume increase ($\Delta V/V_0$) was measured and also estimated using the relationship suggested by Affoune et al. [23], which considers that the Nafion® and the solvent volumes are additive,

$$\Delta V/V_0 = (m_{\text{sol}}/\rho_{\text{sol}})/(m_{\text{Nafion}}/\rho_{\text{Nafion}}), \quad (1)$$

where ΔV is the change in volume and V_0 is the initial resin volume. The densities at 20 °C of Nafion®, methanol, water, triacetin, and olive oil used were 2.1, 0.79, 1, 1.15, and 0.92 g/cm^3, respectively. The results obtained using Eq. (1) and particle dimensions were in good agreement (see Table 2), with volume increase in the order methanol ≫ water > triacetin ≈ olive oil. Comparable results have been obtained for Nafion 117 membranes [22]. The resin treated in methanol resulted in the highest degree of swelling as a result of physicochemical changes (i.e., stretching of the polymer chains leading to higher volumes). Water showed a moderate capability for swelling the resin, which is advantageous from the standpoint of greater acid site accessibility. However, water may also lower the acid strength of the active sites [24] or cause deactivation via hydrolysis (formation of sulfuric acid), as has been suggested for related sulfonic acid catalytic materials (Amberlyst® 15) [25]. It has been reported that mixtures of short-chain alcohols and water cause a greater degree of swelling than either the short-chain alcohol or water alone [22]. THF/water mixtures provide the greatest degree of swelling of the Nafion® resin (as communicated by DuPont).

Both short-chain (triacetin) and long-chain (olive oil) triglycerides showed essentially no swelling capability for the perfluorinated resin; which is analogous to the swelling characteristics obtained with free fatty acids, such as oleic acid [26]. A change in color from transparent to dark amber was observed when Nafion® NR50 was soaked in either short-chain or long-chain triglycerides, indicating the presence of possible side reactions (formation of carbonaceous deposits).

3.1.3. Concentration of acid sites

The initial sulfur content of the resins as determined by elemental analysis was 0.42 and 3.02 wt% for Nafion® SAC-13 and Nafion® NR50, respectively. These values were used to estimate the maximum potential number of available acid sites, as there is one mole of H^+ per mole of S (–$CF_2CF_2SO_3H$). The acid site densities obtained via this method were 131 μmol/g and 939 μmol/g for Nafion® SAC-13 and Nafion® NR50, respectively.

Table 3
Reported and measured acid site densities

Technique	Nafion® SAC-13 (μmol/g)	Nafion® NR50 (μmol/g)
Pulse ammonia chemisorption	412[a]	37 (not swelled)
S elemental analysis	131 ± 3	939 ± 20
Titration	144 ± 7	1104 ± 7
TGA	138 ± 3	–
Manufacturer	>150	>800

[a] Overestimated due to adsorption on SiO_2.

The acid site density calculated from the titration method was 144 ± 7 μmol/g for Nafion® SAC-13 and 1104 ± 7 μmol/g for Nafion® NR50, whereas the acid sites densities measured using pulsed NH_3 chemisorption were 412 μmol/g for Nafion® SAC-13 and 37 μmol/g for Nafion® NR50. Note that there is a significant difference between the acid site densities measured by titration and NH_3 chemisorption methods for the two catalysts. Interestingly, the number of acid sites measured using titration and elemental analysis were in good agreement. Thus, this data suggests that pulse NH_3 chemisorption provides an overestimation of the real number of sites for Nafion® SAC-13, probably because of the ability of silanol groups (on the SiO_2 support) to weakly adsorb the titrating agent. To test this hypothesis, the titration method was repeated leaving the catalyst in solution before titrating with the aqueous NaOH solution (0.05 N). The number of sites measured using this variation in the methodology was 495 ± 26 μmol/g, indicating that the earlier suggestion about silanol groups with the ability to weakly adsorb titrating agents is correct. Thus, the concentration of sites used in further calculations for Nafion® SAC-13 was an average value of 138 μeq H^+/g. For Nafion® NR50, the large difference in number of sites measured by both methods can be explained by increased exposure of catalytic sites on contacting with water due to polymer swelling as shown in the previous section. The fact that NH_3 pulse chemisorption measures such a low value for Nafion® NR50 (∼4% of the expected from the Nafion® sulfur content) is perfectly logical because there is no polymer swelling when exposed to the gas phase. The NH_3 acid site accessibility issue was recently addressed by Siril et al. [27] when comparing macroporous Amberlyst® 15 and gel-type C100H (Purolite). These authors observed that NH_3 adsorption measurements for gel-type resins resulted in a prediction of less than 10% of the real acid site density, which makes the value obtained by this means highly dependent on the catalyst particle size. A summary of the measured acid site densities of the resin catalysts is given in Table 3.

3.1.4. Thermogravimetric analysis

The catalyst resin load, thermal stability, and degradation behavior can be determined using thermogravimetric analysis. Fig. 3 shows the TGA results and the rates of decomposition

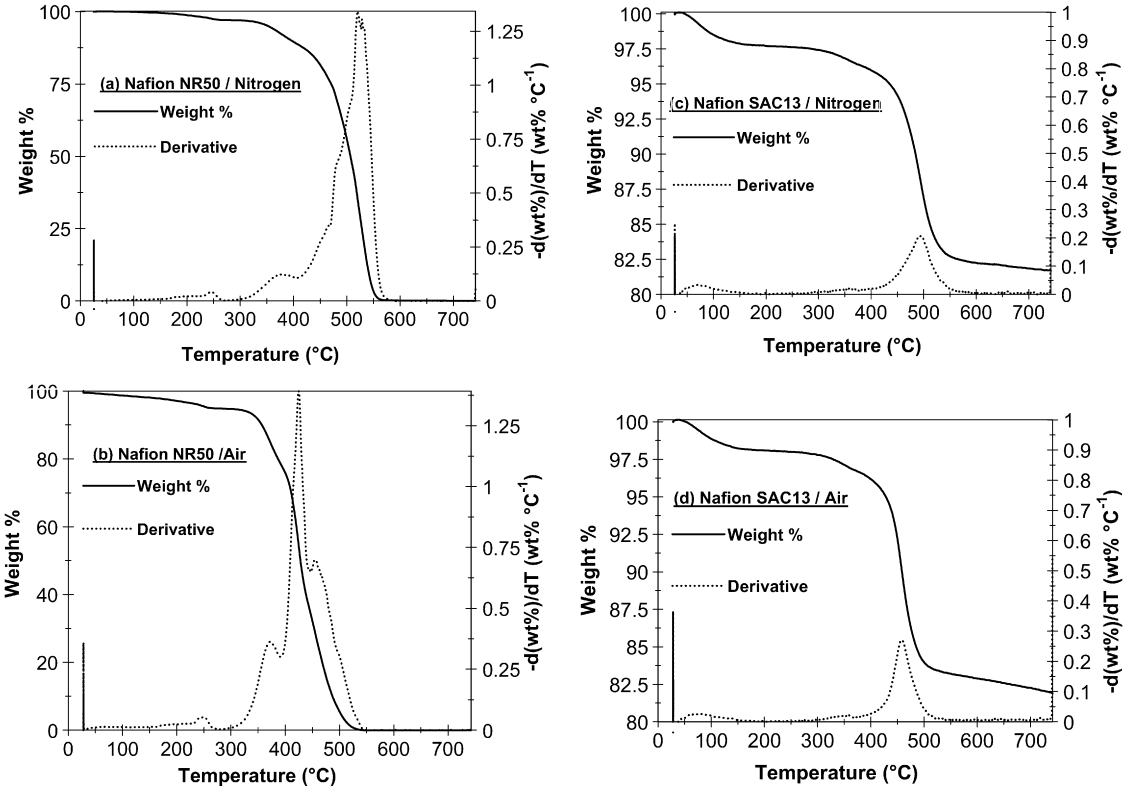

Fig. 3. Weight loss and derivative of weight loss with respect to temperature: (a) Nafion® NR50 in nitrogen, (b) Nafion® NR50 in air, (c) Nafion® SAC-13 in nitrogen, (d) Nafion® SAC-13 in air.

(derivative) for Nafion® NR50 and Nafion® SAC-13 under both UHP nitrogen and air (zero grade) atmospheres. For Nafion® NR50, TGA analysis revealed that there was an initial weight loss (below 250 °C), almost certainly due to the loss of adsorbed water [28]. The thermal decomposition of the pure resin was complete, on being heated in nitrogen, by 580 °C (Fig. 3a); whereas, the resin was fully decomposed by 540 °C when air was used (Fig. 3b). Note that the temperature for the maximum rate of polymer decomposition was decreased by about 105 °C for Nafion® NR50 under the air environment. Thus, the presence of oxygen had a negative effect on catalyst thermal stability.

Nafion® SAC-13 had an initial weight loss of about 2 wt% below 150 °C (Figs. 3c and 3d), which is attributable to the loss of adsorbed water. Comparison of the initial (after weight loss due to moisture <200 °C) and final (after polymer decomposition) sample weights suggests that the resin loading was about 14.7 wt%, which is in agreement with the loading range reported by the manufacturer (10–20 wt%). The decrease in weight for Nafion® SAC-13 observed at temperatures greater than 550 °C (by comparison to the pure resin) is attributable to silica dehydroxylation, by loss of water from surface silanol groups (Si–O–H). TGA results are in good agreement with the previously reported thermal stability and degradation behavior of Nafion® [10,13,28].

The intrinsic thermal stability of the resin for both solid catalysts was found to be the same, 280 °C (<5% resin loss). The temperature at which Nafion® SAC-13 structure begins to collapse (according to manufacturer) is about 200 °C. Therefore, Nafion® -based catalysts cannot be calcined (especially in oxygen and for $T > 200$ °C). Nevertheless, this relatively high temperature stability makes Nafion® catalysts attractive for biodiesel synthesis. The reaction temperatures used when using solid catalysts may have to be higher than that for the traditional alkali-catalyzed ones (⩽60 °C) to compensate for the slower reaction rate per weight of catalyst. For instance, reaction temperatures of 120, 200, and 250 °C have been reported when using propylsulfonic acid-functionalized silicas [18], mixed oxides (Al and Zn) [29], and WZA [30] catalysts, respectively. Reaction temperatures below 250 °C are desirable to avoid side reactions, such as alcohol etherification [31]. Other solid resins, such as Amberlyst® 15 have been shown to be effective for catalyzing biodiesel forming reactions [15,32]; however, the thermal stability for these polystyrene-based ion-exchange resins is relatively poor (maximum operating limit equal to 120 °C).

3.1.5. Scanning electron microscopy

A scanning electron microscopy image of Nafion® SAC-13 dried for analysis shows the morphology of the porous silica matrix (Fig. 4). The pseudospherical particles of silica, which are approximately 3–6 nm in diameter, were present as agglomerates with an overall diameter of about 20–60 nm. The formation of these catalyst particle agglomerates was likely the result of the sample being dried for SEM analysis. Thus, it can be expected that the size of these agglomerates in the reaction media would have been smaller (if they existed at all) than those observed by SEM. Similar images of these types of materials

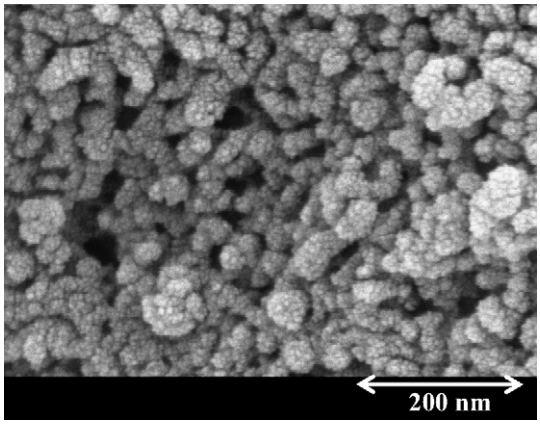

Fig. 4. SEM of Nafion® SAC-13.

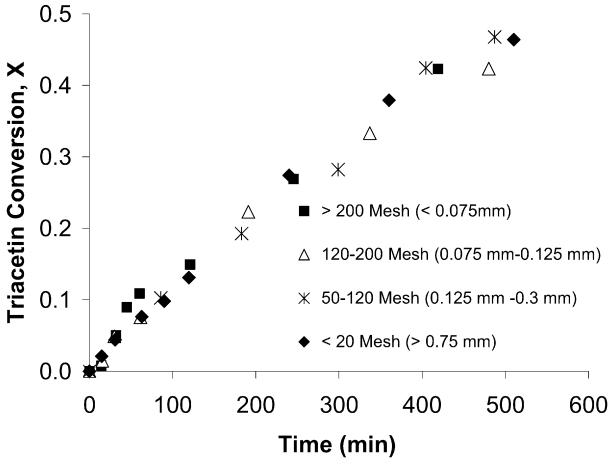

Fig. 5. Variation of triacetin conversion with Nafion® SAC-13 particle size ($C_{TA,0} = 2.3$ M and $C_{MeOH,0} = 13.8$ M at 60 °C and 2 wt% catalyst load).

have been previously obtained using optical microscopy, SEM, and TEM (resin and support) [10,13].

3.2. Diffusional resistances

To ensure that the observed kinetics were attributable to those of the transesterification reaction and not the result of external or internal mass transfer limitations, reaction studies were conducted with varying degrees of agitation and for a range of catalyst particle sizes. For all of these studies, the reactant mixture contained a 6:1 methanol-to-triacetin molar ratio, and the reaction temperature was 60 °C.

3.2.1. External diffusion

External mass transfer limitations on reaction rate were evaluated by conducting reaction experiments at different agitation rates ($N = 134$, 394, 1283, and 2385 rpm). For these studies, the catalyst particle size used was +200 mesh (<0.075 mm). The stirrer speed beyond which there was no effect on reaction rate was considered to be the minimum stirrer speed required to eliminate external diffusion effects. Results showed that external diffusion control was negligible (<5%) for stirrer speeds greater than 800 rpm (data not shown). For stirrer speeds greater than 1283 rpm, no external mass transfer effects were observed. For all of the reaction kinetic studies reported, a stirrer speed of 1790 rpm was used. This high agitation speed ensured that the catalyst was well distributed in the reactor, improved heat transfer within the solution, and reduced the presence of dead zones. For this system, the Reynolds number can be estimated by

$$\mathrm{Re} = \frac{\rho D^2 N}{\mu}, \tag{2}$$

where ρ is the density of the liquid (952 kg/m^3), D is the impeller diameter (0.02 m), N is the angular velocity of the impeller (29.8 rps), and μ is the viscosity of the liquid (8.3×10^{-4} Pa s), as measured using an Ubbelohde viscometer. For the conditions used (60 °C), N_{Re} was equal to 13,650.

3.2.2. Internal diffusion

The presence of internal diffusion limitations on reaction rate was examined for the porous catalyst, Nafion® SAC-13. Samples with different average particle sizes (0.075–0.75 mm) were used in the experiment. Neglecting any volume change with reaction (liquid phase), the conversion of triacetin (X) is given by

$$X = 1 - C_{TG}/C_{TG,0}, \tag{3}$$

where C_{TG} and $C_{TG,0}$ are the triacetin molar concentrations at a particular time and initially, respectively. Equivalent reaction conversions were achieved in the same amount of time for systems with catalyst particles <0.75 mm (Fig. 5) even for conversions <10%. This suggests that internal diffusion limitations were not important for any particle size used in this study; however, the selectivity to final products (i.e., glycerol) was higher for the larger catalyst particles. One speculative possibility is that the glyceride molecules diffusing into the larger Nafion® SAC-13 particles had a greater probability for the series reaction to occur before the glycerol-containing molecule diffused back out of the catalyst particle. To avoid any internal mass transfer effects, all further reactions were carried out with catalyst particles >200 mesh (<0.075 mm) for Nafion® SAC-13 unless otherwise stated.

3.3. Effect of reactant preexposure on initial catalyst activity

Because the physicochemical properties of Nafion® are significantly affected by activation conditions (namely, reactant preexposure), a comparison of the initial transesterification activity was investigated as a function of different reaction startups. Insignificant initial reaction rate differences were observed for Nafion® SAC-13 (Fig. 6), regardless of the order of mixing the catalyst with the reactants, due in large part to the higher dispersion of the Nafion® resin and the lack of need for polymer swelling.

As one would expect from the pure perfluorinated resin swelling experiments, the initial activity (on a weight basis) for Nafion® NR50 precontacted with the methanol reactant was found to be substantially higher (4–5 times) than that for the dry catalyst added directly to the reaction mixture. It can be inferred that the low activity observed with the dry catalyst resulted from

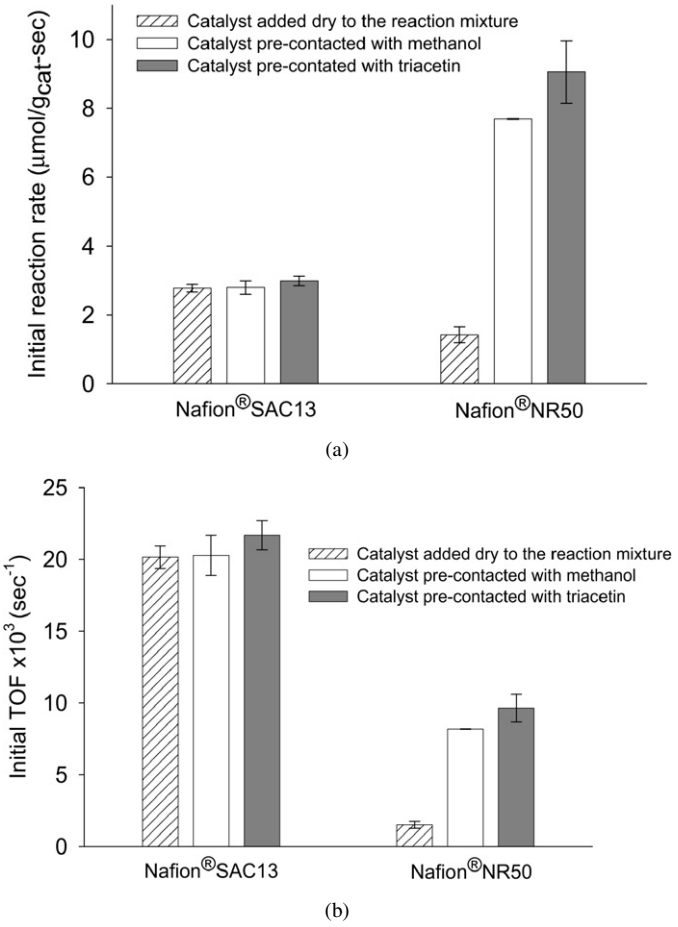

Fig. 6. Effect of catalyst preswelling (in different solvents) prior to reaction on the initial transesterification rate (conversion $\leqslant$10%) on a catalyst (a) weight basis (catalyst loading = 2 wt%) and (b) site basis ($C_{\text{cat,SAC-13}} = 138$ μmol/g and $C_{\text{cat,NR50}} = 939$ μmol/g).

reaction occurring only on the outermost surface, which at the beginning of the reaction presents only a moderate number of active sites. However, it is not obvious why the catalyst precontacted with triacetin, when the degree of resin swelling was insignificant (Table 2), led to a similar reaction rate as for the catalyst precontacted with methanol. Similar observations have been obtained for the preparation of monoglycerides; the reaction rate showed an enhancement by precontacting oleic acid with the resin (Amberlyst 31, Amberlyst 16, and K1481) before reaction with glycerol, even when the extent of swelling of these resins was shown to be insignificant.

A more comprehensive comparison of the catalyst activities can be done on a rate per-site basis (TOF) rather than a rate/g catalyst basis (Fig. 6b). One might expect that TOFs on Nafion® SAC-13 and Nafion® NR50 would be similar because the active materials are similar. The acid strength reported in the literature for Nafion® NR50 ($H_0 \sim -10$ to -12 [33]) appears to be somewhat higher than that of Nafion® SAC-13 ($H_0 > -12$ [10]), probably as a result of the interaction between the support silanol groups and the highly dispersed resin [34]. Thus, if all potential sites were available, then the TOF for Nafion® NR50 likely would be higher. But this is not the case—in fact, the TOF is 60–70% lower than Nafion® SAC-13. This leads us to suggest that even with precontacting with methanol or triacetin, many of the Nafion® NR50 sites are not available for reaction. It is clear that a more efficient utilization of the resin sites, due to greater accessibility of the reacting molecules to the active sites, is achieved when the resin is highly dispersed as a nanocomposite (Nafion® SAC-13).

3.4. Reaction rate expressions and activation energies

To determine an appropriate reaction model for the conversion of triglycerides, Nafion® SAC-13 was used because it has been shown to not have the swelling issues associated with Nafion® NR50. The reaction temperature was held constant (60 °C) to permit calculation of the apparent reaction orders with respect to triacetin and methanol, α and β, respectively. These reaction orders were obtained by varying one reactant concentration (MeOH = 0.67–5.2 M or TA = 1.2–2.6 M) while keeping the other reactant concentration constant and in excess. The power rate law model can be written as

$$-r_0 = kC_{\text{cat}}C_{\text{TG},0}^{\alpha}C_{\text{MeOH},0}^{\beta}, \tag{4}$$

where k is the reaction rate constant and C_{cat} is the catalyst concentration ($C_{\text{cat,SAC-13}} = 2.7$ meq $H^+/L_{\text{reaction volume}}$). r_0 represents the initial reaction rate (<5% triacetin conversion), $C_{\text{TG},0}$ and $C_{\text{MeOH},0}$ are the initial triglyceride and methanol concentrations, respectively.

The apparent reaction orders for the triglyceride ($\alpha_{\text{SAC-13}} = 0.90$) and the alcohol ($\beta_{\text{SAC-13}} = 0.88$) were calculated from the slopes of the fitted straight lines in Figs. 7a and 7b, with correlations for the fitted lines of 0.99 and 0.98, respectively. In addition, k can be determined from the y-intercept of the fitted lines and was determined to be $k_{\text{SAC-13,60 °C}} = 0.050 \pm 0.003$ $L^{1.8}/(\text{min mol}^{1.8})$ for Nafion® SAC-13. For H_2SO_4 catalysis, both triacetin ($\alpha_{H_2SO_4} = 1.02$) and methanol ($\beta_{H_2SO_4} = 1.00$) exhibited first-order behavior, as expected from the hypothesized mechanism and the rate-limiting step (RLS) [7]. (The goodness of fit in determining α and β was >0.99.) The value obtained for k using $C_{\text{cat},H_2SO_4} = 7.5$ meq $H^+/L_{\text{reaction volume}}$ was $k_{H_2SO_4,60\,°C} = 0.064 \pm 0.015$ $L^2/(\text{min mol}^2)$, similar to that obtained for Nafion® SAC-13.

The effect of reaction temperature was investigated in the 30–60 °C temperature range. The activation energies (E_{app}) were estimated from the Arrhenius plots shown in Fig. 8. E_{app} for the conversion of triacetin to diacetin using Nafion® SAC-13 was found to be 48.5 ± 1.6 kJ/mol, whereas the E_{app} for the H_2SO_4 catalyzed reaction was 46.1 ± 2.1 kJ/mol. This result corroborates our previous observation about the reaction not being mass transfer-limited when catalyzed by the nanocomposite.

3.5. Selective poisoning of Nafion® SAC-13 Brønsted acid sites

To obtain more insight into the acid resin-catalyzed transesterification mechanism, selective poisoning of the Brønsted acid sites in Nafion® SAC-13 was performed using pyridine (an organic base) [35]. Before reaction, 1 g of Nafion® SAC-13

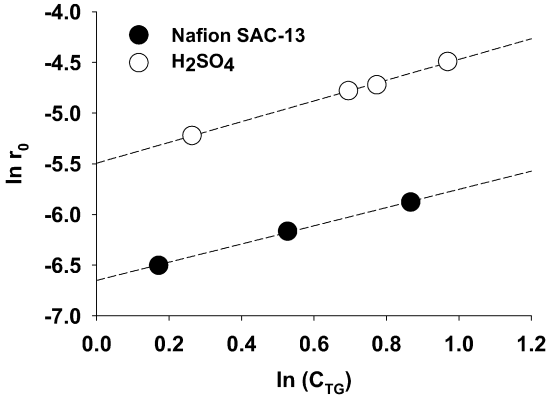

(a)

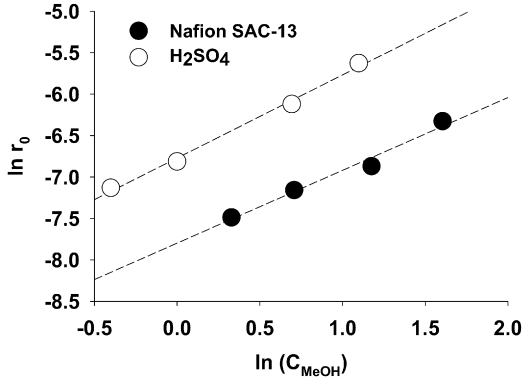

(b)

Fig. 7. Effect of reactant concentration on initial reaction rate (conversion ⩽5%) at 60 °C: (a) triacetin ($C_{MeOH,0} = 13.8$ M) and (b) methanol ($C_{TA,0} = 2.3$ M).

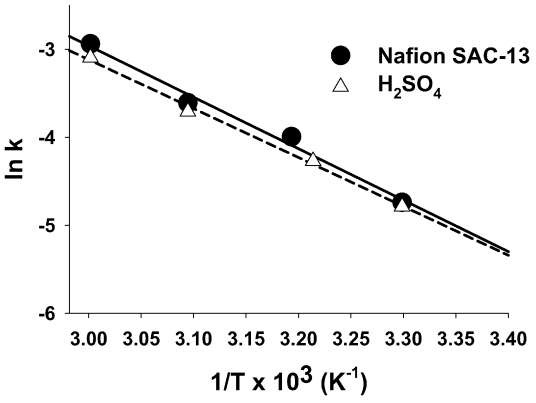

Fig. 8. Arrhenius plot for the transesterification of triacetin to diacetin using Nafion® SAC-13 and H_2SO_4 catalysts. Temperature range 30–60 °C and triacetin conversion ⩽10%.

was added to a known concentration of pyridine in methanol. Poisoning was allowed to proceed for 48 h at 60 °C with continuous stirring (150 rpm) to guarantee equilibration of the pyridine with the catalytic sites. Then the reaction was carried out. The results show that the reaction rate dropped linearly with increasing pyridine concentration (Fig. 9). This result indicates that the RLS involves a single reaction site.

The pyridine poisoning experiments also confirmed the previously given estimations of the concentration of active sites available on Nafion® SAC-13. Examination of Fig. 9 reveals

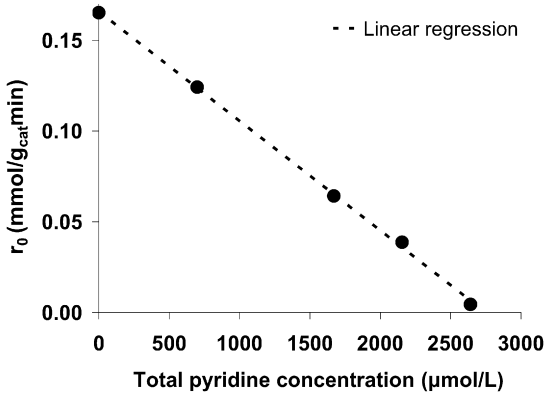

Fig. 9. Selective poisoning of the Brønsted acid sites on Nafion® SAC-13 using pyridine adsorption ($C_{TA,0} = 2.3$ M and $C_{MeOH,0} = 13.8$ M at 60 °C and 2 wt% catalyst load).

that zero activity was manifested when the poison concentration was equivalent to 2764 μeq H^+/L, which is comparable (only 3% different) to the estimated concentration of sites, 2680 μeq H^+/L ($C_{cat} = 138$ μeq H^+/g), based on *S* elemental analysis, site titration, and TGA (see Table 3).

3.6. Proposed mechanism for solid acid-catalyzed transesterification of triglycerides

Although the catalytic activity of solid acid catalysts like Amberlyst® 15 [32], WZA [30], SO^{4-}/SnO_2, and SZ [16] have been investigated for triglyceride transesterification in recent years, the complexity of the vegetable oil mixtures used and the difficulty in obtaining good initial rate data (due to 2-liquid phase behavior) [5] has made the study of the mechanistic pathway extremely challenging. In contrast, use of a model triglyceride such as triacetin as the sole triglyceride for reaction in a detailed kinetic study permits us to form a hypothesis about the solid acid-catalyzed transesterification mechanism.

It is generally accepted that homogeneous acid-catalyzed transesterification is initiated via the protonation of the triglyceride carbonyl moiety, followed by the nucleophilic attack of the alcohol to the protonated triglyceride, and finally proton migration and breakdown of the intermediate (to form the diglyceride) [7,36]. The cycle is repeated for the intermediate products. Because the RLS appears to be the second one, both reaction orders (with respect to the glyceride and the alcohol) are equal to 1. However, in most investigations dealing with acid catalysis, a much larger excess of methanol (≫6:1 methanol:TG) is used to compensate for the slower reaction rate [14]. As may be expected, under those conditions the apparent reaction order with respect to methanol goes to zero ($\beta \to 0$) [37].

Both Nafion® SAC-13 and H_2SO_4 catalysts have only Brønsted acidity and have similar acid site strengths based on the Hammett indicator method: $H_{0,SAC\text{-}13} > -12$ and $H_{0,H_2SO_4} = -12$ [10]. The fact that both reaction orders with respect to glyceride and alcohol are close to first order for Nafion® SAC-13 is indicative that surface reaction is the RLS. In this study, the selective poisoning of sites with pyridine provided

Table 4
Scheme for the conversion of triglycerides to diglycerides (neglecting the other reactions in the series)

Step		$k(\rightarrow)$	$k_{-}(\leftarrow)$	$K = k/k_{-}$
(1) Triglyceride ad/desorption	$TG + S \leftrightarrow TG{\cdot}S$	k_{TG}	k_{-TG}	K_{TG}
(2) Methanol ad/desorption	$MeOH + S \leftrightarrow MeOH{\cdot}S$	k_{MeOH}	k_{-MeOH}	K_{MeOH}
(3) Surface reaction (RLS)	$TG{\cdot}S + MeOH \rightarrow E{\cdot}S + DG$	k_s	k_{-s}	K_s
(4) Ester ad/desorption	$E{\cdot}S \leftrightarrow E + S$	k_e	k_{-e}	K_e
Overall reaction	$TG + 2MeOH + S \leftrightarrow DG + E + MeOH{\cdot}S$			

Note. Here S represents the vacant acid sites, E denotes the ester (i.e., methyl acetate); TG·S, MeOH·S, and E·S designate the adsorbed species; and K and k stand for the equilibrium and reaction rate constants, respectively.

evidence that the RLS involves a single reaction site. Consequently, there exist two possibilities: either the reaction proceeds via a protonated triglyceride or a protonated alcohol intermediate. For the solid-acid-catalyzed esterification reaction, most investigators have found that the carboxylic acid first adsorbs on the catalytic surface and then reacts with bulk phase alcohol [38–41]. This mechanism discrimination procedure has led us to suggest that the homogeneous and the heterogeneous catalyzed reactions are likely following a similar mechanism. Thus, if we assume that the reaction pathway for the conversion of triglyceride to diglyceride on Nafion® SAC-13 mainly resembles the homogeneous one, then surface reaction between the protonated triglyceride and bulk alcohol would be the RLS. Although the mechanism for reaction requires the triglyceride to first adsorb followed by an Eley–Rideal-type reaction with methanol from the liquid phase, the competitive adsorption on the reaction sites of the alcohol (i.e., methanol) must also be included based on the order of reaction of methanol being <1. Therefore, the scheme for the conversion of triglycerides to diglycerides (neglecting the other reactions in the series) can be represented by Table 4.

Based on Langmuir–Hinshelwood kinetics with surface reaction being the RLS, the observed reaction would be

$$r_s = k_s\left(C_{TG{\cdot}S}C_{MeOH} - \frac{C_{E{\cdot}S}C_{DG}}{K_s}\right). \tag{5}$$

Initially, when the concentration of products can be neglected, Eq. (5) reduces to

$$r_{s,0} = k_s(C_{TG{\cdot}S}C_{MeOH}). \tag{6}$$

The concentrations of the adsorbed species can be obtained considering that the reaction rate constant for the formation of the intermediates is large compared to the reaction rate ($r_{TG}/k_{TG} \approx r_{MeOH}/k_{MeOH} \approx 0$, i.e., pseudoequilibrium). Therefore,

$$C_{TG{\cdot}S} = K_{TG}C_{TG}C_s \tag{7}$$

and

$$C_{MeOH{\cdot}S} = K_{MeOH}C_{MeOH}C_s. \tag{8}$$

Substituting Eq. (7) into Eq. (6) gives

$$r_{s,0} = k_s(K_{TG}C_{TG}C_sC_{MeOH}). \tag{9}$$

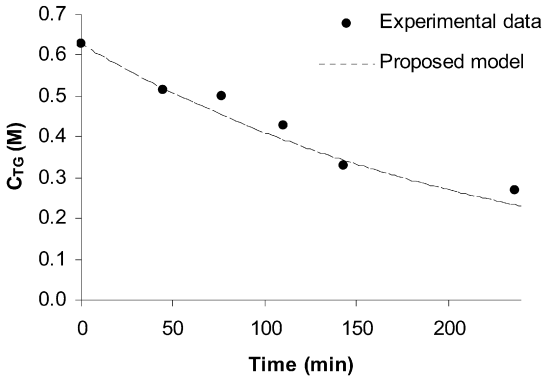

Fig. 10. Comparison of experimental data results for the conversion of triacetin to diacetin to the model obtained using the proposed mechanistic pathway (reaction temperature 60 °C).

Finally, the concentration of vacant sites (C_s) can be easily obtained from the site mass balance to give

$$r_{s,0} = \frac{k_sC_{cat}K_{TG}C_{TG}C_{MeOH}}{1 + K_{TG}C_{TG} + K_{MeOH}C_{MeOH}}. \tag{10}$$

Note that Eq. (10) deviates from the classical Eley–Rideal bimolecular expression [42], as it includes the competitive methanol adsorption term ($K_{MeOH}C_{MeOH}$) in the denominator. Further rearrangements of Eq. (10) enable estimation of the equilibrium constants by varying one reactant concentration and keeping the other reactant concentration constant. The values obtained were $K_{TG} = 0.14\ M^{-1}$ and $K_{MeOH} = 0.10\ M^{-1}$, which are very similar, as expected from the reaction orders. Likewise, the k_s value was obtained from the y-intercept of the linearized equations derived from Eq. (10) and was estimated to be $k_s = 0.71 \pm 0.04$ L/(eq min). To validate the proposed model, a different set of experimental data was fit using $C_{cat} = 0.016$ eq H^+/L, $C_{TG} = 0.63$ M, and $C_{MeOH} = 3.81$ M. The solution of Eq. (10) can be easily obtained using any ordinary differential equations solver program, such as MATLAB and Polymath. Here, we used Polymath 5.1 RKF45 function. As shown in Fig. 10, the derived model (dashed line) was able to effectively predict the experimental conversion of triacetin to diacetin.

3.7. Catalyst deactivation and reusability

Three consecutive 2-h transesterification reaction cycles were used to determine the extent of Nafion® SAC-13 deactivation. To facilitate catalyst recovery, the catalyst was used in its

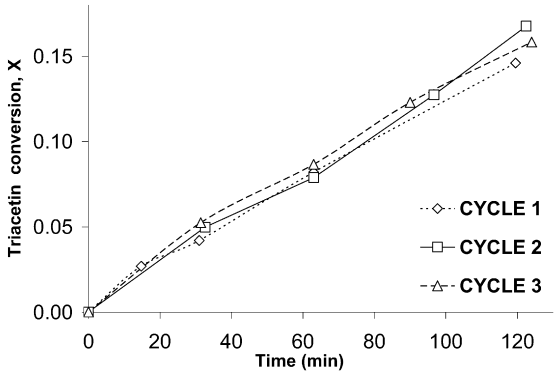

(a)

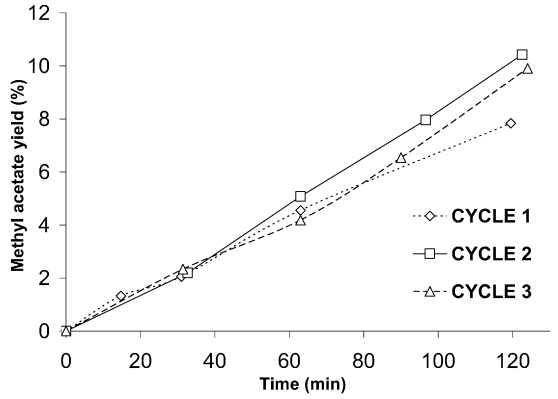

(b)

Fig. 11. Nafion® SAC-13 activity during multiple triacetin transesterification reaction cycles with decantation of the reaction mixture solvent between cycles: (a) triacetin conversion and (b) methyl acetate yield.

pellet form. The variation in triacetin conversion and methyl acetate yield between runs was insignificant, as shown in Fig. 11. The fact that the catalyst showed the same activity through multiple cycles also indicates that the reaction was truly heterogeneously catalyzed (i.e., no leaching out into the liquid phase of the catalytic species). Nafion® SAC-13 was resieved after reaction; the results indicated that attrition was not significant during these runs. For the pure resin, Nafion® NR50 (added dry to the reaction mixture), the catalytic activity increased after the first 2 h reaction cycle because of swelling [15].

4. Conclusion

To evaluate the possibility of replacing homogeneous catalysts with solid acids in the synthesis of biodiesel from free fatty acid-containing feedstocks, a fundamental investigation of the kinetics of transesterification of triacetin with methanol was carried out for perfluorinated resin catalysts, and the results were then compared with the kinetics of H_2SO_4. The activity for transesterification of Nafion® NR50 was found to strongly depend on the reactants' accessibility to the acid sites. The pure resin exhibited the greatest degree of swelling after pretreatment in methanol (relative to other components in the system), thereby exposing more sites for reaction. On the other hand, Nafion® SAC-13 showed no dependence of catalytic activity on solvent precontacting and also more efficient use of the resin acid sites (i.e., unrestricted accessibility of the reacting molecules to the active sites).

Based on kinetic analysis, the similarities found between solid and liquid catalysts (in terms of activation energies and reaction orders) and the variations in catalyst activity after the selective poisoning of Brønsted acid sites in Nafion® SAC-13, a mechanistic pathway similar to that for homogeneous acid catalysts was proposed. To the best of our knowledge, this is the first time that a mechanism has been proposed for the solid acid-catalyzed transesterification of triglycerides. This mechanism consists of a triglyceride protonation step, followed by surface reaction between the protonated triglyceride and liquid-phase alcohol (which is the RLS) and then a product desorption step. A deviation from the classical Eley–Rideal bimolecular mechanistic expression is obtained due to competitive adsorption of methanol on the resin acid sites. This mechanistic model was shown to successfully predict the conversion of triglycerides to diglycerides. No catalyst deactivation was found under the conditions of this study.

Acknowledgments

The authors thank the U.S. Department of Agriculture (Award No 68-3A75-3-147) for financial support. They also thank Dan Sweeney, Clemson University for assisting with the TGA.

References

[1] G. Vicente, M. Martínez, J. Aracil, A. Esteban, Ind. Eng. Chem. Res. 44 (2005) 5447.
[2] E. Lotero, J.G. Goodwin Jr., D.A. Bruce, K. Suwannakarn, Y. Liu, D.E. Lopez, in: J. Spivey, K.M. Dooley (Eds.), The Catalysis of Biodiesel Synthesis, vol. 19, Royal Chem. Soc. Publishing, Cambridge, UK, 2006.
[3] B. Freedman, R.O. Butterfield, E.H. Pryde, J. Am. Oil Chem. Soc. 63 (1986) 1375.
[4] G. Vicente, M. Martinez, J. Aracil, Bioresour. Technol. 92 (2004) 297.
[5] V. Mao, S.K. Konar, D.G.B. Boocock, J. Am. Oil Chem. Soc. 81 (2004) 803.
[6] H. Noureddini, D. Zhu, J. Am. Oil Chem. Soc. 74 (1997) 1457.
[7] E. Lotero, Y. Liu, D.E. Lopez, K. Suwannakarn, D.A. Bruce, J.G. Goodwin Jr., Ind. Eng. Chem. Res. 44 (2005) 5353.
[8] M.G. Kulkarni, A.K. Dalai, Ind. Eng. Chem. Res. 45 (2006) 2901.
[9] R. Tesser, M. Di Serio, M. Guida, M. Nastasi, E. Santacesaria, Ind. Eng. Chem. Res. 44 (2005) 7978.
[10] M.A. Harmer, Q. Sun, Appl. Catal. A Gen. 221 (2001) 45.
[11] M.A. Harmer, Q. Sun, A.J. Vega, W.E. Farneth, A. Heidekum, W.F. Hoelderich, Green Chem. 2 (2000) 7.
[12] T.A. Nijhuis, A.E.W. Beers, F. Kapteijn, J.A. Moulijn, Chem. Eng. Sci. 57 (2002) 1627.
[13] M.A. Harmer, W.E. Farneth, Q. Sun, J. Am. Oil Chem. Soc. 118 (1996) 7708.
[14] M. Mittelbach, A. Silberholz, M. Koncar, Novel aspects concerning acid catalyzed alcoholysis of triglycerides, Oils–Fats–Lipids 1995, Proceedings of the 21st World Congress of the International Society for Fats Research, The Hague, 1996, p. 497.
[15] D.E. López, J.G. Goodwin Jr., D.A. Bruce, E. Lotero, Appl. Catal. A Gen. 295 (2005) 97.
[16] J. Jitputti, B. Kitiyanan, P. Rangsunvigit, K. Bunyakiat, L. Attanatho, P. Jenvanitpanjakul, Chem. Eng. J. 116 (2006) 61.
[17] A.A. Kiss, A.C. Dimian, G. Rothenberg, Adv. Synth. Catal. 348 (2005) 75.

[18] I.K. Mbaraka, K.J. McGuire, B.H. Shanks, Ind. Eng. Chem. Res. 45 (2006) 3022.
[19] T. Ebiura, T. Echizen, A. Ishikawa, K. Murai, T. Baba, Appl. Catal. A Gen. 283 (2005) 111.
[20] C. Park, M.A. Keane, J. Mol. Catal. A Chem. 166 (2001) 303.
[21] F.J. Waller, R.W. Van Scoyoc, CHEMTECH 17 (1987) 438.
[22] G. Gebel, P. Aldebert, M. Pineri, Polymer 34 (1992) 333.
[23] A.M. Affoune, A. Yamada, M. Umeda, J. Power Sources 148 (2005) 9.
[24] Y. Liu, E. Lotero, J.G. Goodwin Jr., J. Mol. Catal. A Chem. 245 (2005) 132.
[25] J.M. Aragón, M.M.R. Vegas, L.G. Jodra, Ind. Eng. Chem. Res. 33 (1994) 592.
[26] Y. Pouilloux, S. Abro, C. Vanhove, J. Barrault, J. Mol. Catal. A Chem. 149 (1999) 243.
[27] P.F. Siril, D.R. Brown, J. Mol. Catal. A Chem. 252 (2006) 125.
[28] S.R. Samms, S. Wasmus, R.F. Savinell, J. Electrochem. Soc. 143 (1996) 1498.
[29] L. Bournay, D. Casanave, B. Delfort, G. Hillion, J.A. Chodorge, Catal. Today 106 (2005) 190.
[30] S. Furuta, H. Matsuhashi, K. Arata, Catal. Commun. 5 (2004) 721.
[31] D. Ballerini, G. Hillion, l'Actualité Chim. 11–12 (2002) 64.
[32] S.C.M. dos Reis, E.R. Lachter, R.S.V. Nascimento, J.A.J. Rodriguez, M. Garcia Reid, J. Am. Oil Chem. Soc. 82 (2005) 661.
[33] G.A. Olah, G.K.S. Prakash, J. Sommer, Superacids, vol. 58, Wiley, New York, 1985.
[34] P. Botella, A. Corma, J.M. López-Nieto, J. Catal. 185 (1999) 371.
[35] J. Macht, C.D. Baertsch, M. May-Lozano, S.L. Soled, Y. Wang, E. Iglesia, J. Catal. 227 (2004) 479.
[36] L.C. Meher, D.V. Sagar, S.N. Naik, Renewable Sustainable Energy Rev. 10 (2006) 248.
[37] S. Zheng, M. Kates, M.A. Dube, D.D. McLean, Biomass Bioenergy 30 (2006) 267.
[38] R. Koster, B. van der Linden, E. Poels, A. Bliek, J. Catal. 204 (2001) 333.
[39] B. Chemseddine, R. Audinos, J. Membrane Sci. 115 (1996) 77.
[40] S.R. Kirumakki, N. Nagaraju, K.V.R. Chary, Appl. Catal. 299 (2006) 185.
[41] A. Corma, H. Garcia, S. Iborra, J. Primo, J. Catal. 120 (1989) 78.
[42] M.A. Vannice, Kinetics of Catalytic Reactions, Springer, New York, 2005, p. 172.